PROCEEDINGS

PCF 2014

XIV Portuguese Conference on Fracture

UNIVERSIDADE DE TRÁS-OS-MONTES E ALTO DOURO

utad

PROCEEDINGS

EDITED BY

Abílio de Jesus

Alfredo Ribeiro

José Morais

José Xavier

Nuno Dourado

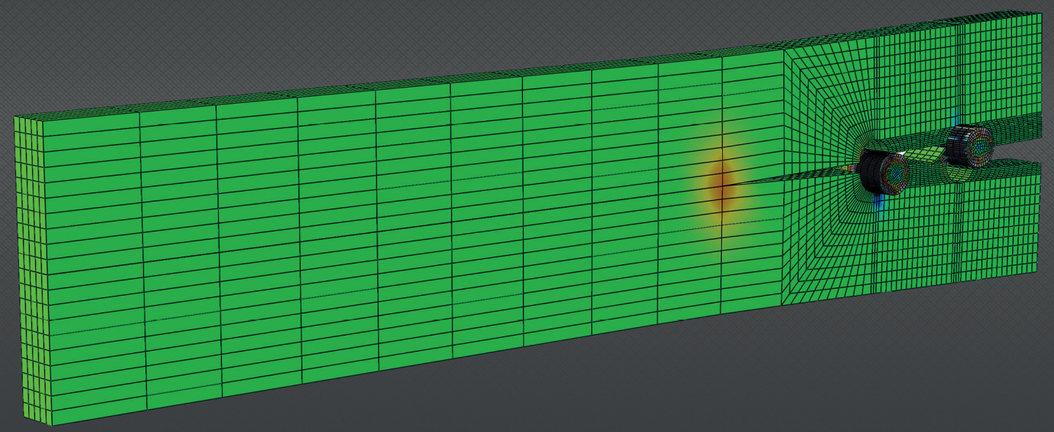

RÉGUA, 6-7TH FEBRUARY, 2014

PCF 2014

XIV Portuguese Conference on Fracture

FRACTURE CHARACTERIZATION OF WOOD UNDER MODE I LOADING USING THE SEN-TPB TEST

N. Dourado[1], M.F.S.F. de Moura[2], S. Morel[3], J.J.L. Morais[1]

[1] Universidade de Trás-os-Montes e Alto Douro, UTAD, CITAB, Departamento de Engenharias, Quinta de Prados, 5000-801 Vila Real, Portugal

[2] Faculdade de Engenharia da Universidade do Porto, Departamento de Engenharia Mecânica, Rua Dr. Roberto Frias, 4200-465 Porto, Portugal

[3] Université de Bordeaux, UMR 5295, Institut de Mécanique et d'Ingénierie – Bordeaux (I2M), Département Génie Civil et Environnemental (GCE), Bordeaux F-33000, France

ABSTRACT

Mode I fracture characterization was induced in wood (*Picea abies* L.) using the single-edge-notched beam loaded in three-point-bending. A developed data reduction scheme based on the equivalent linear elastic fracture mechanics was used to evaluate the *Resistance*-curve instead of classical methods. The method is found on beam theory and crack equivalent concept taking into account the triangular stress relief region that develops in the crack vicinity. The method dispenses crack length monitoring in the course of the loading process, providing a complete *Resistance*-curve which is essential for a clear identification of the fracture energy. The validation of the procedure has been performed numerically using a bilinear cohesive damage model, thus allowing the simulation of both damage initiation and growth. The numerical model also provided the critical specimen dimensions that permit the attainment of accurate evaluation of the fracture toughness in wood.

KEYWORDS: Wood, Mode I, Fracture characterization, Single-edge-notched beam loaded in three-point-bending.

1. INTRODUCTION

Economic and ecological reasons can be pointed as main reasons for the increasing demand of wood in timber constructions. The design of wood structures is frequently performed on the basis of classical strength of materials approaches [1], thus leading to conservative predictions. However, in recent years the development of fracture mechanics concepts, namely the methods based on energetic analysis [2–5], has been contributing to improve the predictions in wood mechanical behaviour. Consequently, the definition of accurate methods to measure wood fracture properties, namely under pure mode I loading, acquires special importance.

Macroscopically, wood is usually regarded as a continuum, homogeneous and orthotropic material, exhibiting three axes of symmetry: longitudinal (L) direction along the fibres, radial (R) and tangential (T), aligned along normal and tangent directions of wood growth rings, respectively (Fig. 1). As a consequence, six fracture propagation systems are defined: TL, RL, LR, TR, RT and LT. According to this notation the first letter indicates the normal direction to the crack plane while the second one gives the direction of crack propagation. The most frequently studied fracture systems in wood are the TL and RL, since cracks in wood are more prone to develop in these directions. Contrarily to the later ones, LR or LT fracture systems are very unlike to occur since it renders impossible to make a crack to develop across wood fibres.

Due to its simplicity and existence of appropriate data reduction schemes [5,6] the Double Cantilever Beam test (DCB) test is especially adequate to perform the characterization of wood under mode I loading. However, this test is only suitable for the RL and TL crack propagation systems owing to the fact that in these cases crack advances along wood fibres. In regard to other fracture systems (i.e., TR and RT) the DCB

is not considered a suitable test since fracture propagation is characterized by a pronounced stick–slip effect. In these later systems the crack tends to deviate from the mid-plane which leads to mixed-mode loading rather than pure mode I.

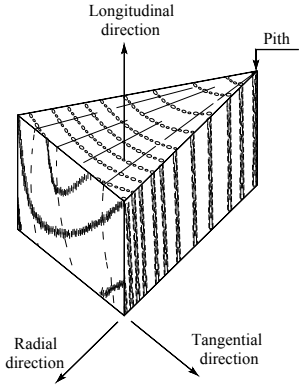

Figure 1. Wood axes: Longitudinal (L), Radial (R) and Tangential (T).

Moreover, due to the curvature of the growth rings it turns impossible to produce DCB specimens for TR and RT fracture systems. Regardless that the material is located sufficiently far from the pith, wood is considered as an orthotropic material when analysed on the macro scale. It is also of great importance that tested wood is free from knots, which frequently poses difficulties for the DCB owing to its length. This fact is of major importance when the size effect study is the goal. In such a case other tests are possible to perform such as the Compact Tension test [7], Wedge Splitting (WS) test [2] and the Single Edge Notched-Three Point Bending (SEN-TPB) test [4, 8, 9] (Fig. 2).

Boström [7] has applied the Compact Tension test (CT) to assess theoretically the initiation and growth of the fracture process zone (FPZ) in wood, being essential to evaluate the critical stress intensity factor in wood. It was concluded that the load-displacement curve is sensitive to the modulus of elasticity perpendicular to wood fibres (grain), as well as the tensile strength, fracture energy and specimen size. The Wedge-Splitting (WS) test has been proposed by Stanzl-Tschegg et al. [2], consisting on a slim (5-10°) wedge and two load transmission parts. The proposed apparatus permit minimizing the energy losses since it uses roll bodies, which render possible to transmit loads from the wedge to the specimen without friction effects. High horizontal load components are obtained from the testing machine leading to stable crack initiation and growth.

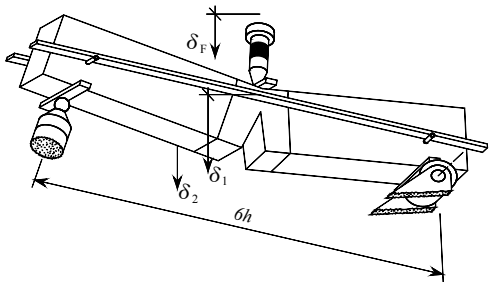

Figure 2. Sketch of SEN-TPB test set-up.

Due to simplicity in specimen production and use of common accessories the single-edge-notched beam loaded in three point bending (SEN-TPB) is easier to execute than the WS test. Besides, one requires relatively small dimensions to get consistent fracture parameters in wood [8]. This is a very important aspect since a specimen has to be free from knots, resin pockets and grain misalignment, in order to get accurate values of fracture energy. The SEN-TPB has been used by Daudeville [9] to evaluate the fracture energy in the RL and TL fracture systems, leading to size effect studies. Later on, Dourado et al. [4] used this specimen geometry to identify cohesive fracture properties in two wood species (*Pinus pinaster* Ait. and *Picea abies* L.), identifying the interaction of the cohesive zone with the specimen boundaries. This phenomenon was observed as playing an important role on the attainment of the self-similar crack propagation, being at the origin of misevaluation of fracture toughness in quasi-brittle failure.

Though presenting a considerable number of advantages over other fracture test, the SEN-TPB has several drawbacks that impede the clear identification of the fracture energy obtained on the basis of classical procedures. The aim of this study is to present a data reduction scheme that permits characterize wood fracture under pure mode I loading using the SEN-TPB. This is accomplished by applying beam theory and crack equivalent concept, which dispenses crack length measurement during its propagation. The procedure considers the existence of a triangular shape stress relief zone in the vicinity of the crack. The method is validated numerically by confirming that fracture energy release rate obtained by the data reduction scheme is equal to the total energy below the damage law used in the cohesive zone modelling. The critical specimen size is determined numerically, and fracture tests were performed to evaluate fracture toughness in *Picea abies* L.

Table 1. Specimen dimensions used in FEA.

Series	h (mm)	L_1 (mm)	L (mm)	a_0 (mm)	b (mm)
D_0	17.5	43.75	52.5	8.75	5
D_1	35	87.5	105	17.5	10
D_2	70	175	210	35	20
D_3	140	350	420	70	40
D_4	280	700	840	140	80
D_5	560	1400	1680	280	160

2. COHESIVE ZONE MODELLING

The adapted SEN-TPB is formed by three wood parts (specimen: central part; lateral segments: remaining two parts) rigidly bonded to constitute a composite beam. Since the aim is to induce fracture under mode I loading in the TL fracture system, a pre-crack (a_0) is fabricated in the central part of the beam. Wood lateral segments are oriented in such a way as to assure high bending stiffness to the beam. The utilization of lateral segments is fundamental to assure the accomplishment of fracture in the TL system in a continuum wood specimen as the loading span gets higher. It should be noted that the adapted SEN-TPB allows performing fracture characterization of wood in other systems (e.g., TR and RT), without size constraints. Following the size relations schematized in Fig. 3, homothetic specimens (Table 1) were numerically analysed to identify the most suitable dimensions to evaluate fracture energy in wood. As noticed by Dourado N. [10] this procedure is crucial in wood fracture mechanics when size effect studies are aimed. Consequently, finite element analysis (FEA) in plane strain assumption combining cohesive zone modelling was performed [11]. Figure 4 shows the developed FE model of the adapted SEN-TPB with uniform ligament discretization (every 0.5 mm). The presented FE-mesh corresponds to series D_2 (Table 1) for an analysis with 837 solid elements (8-node tetrahedral and 6-nodes triangular) with a total of 64 cohesive elements.

Table 2 resumes the set of elastic properties used in the numerical model to simulate the mechanical behaviour of *Picea abies* L. [12].

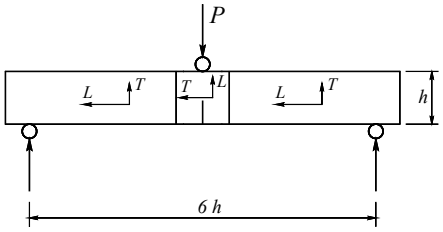

Figure 3. Lay-out of wood parts in the SEN-TPB.

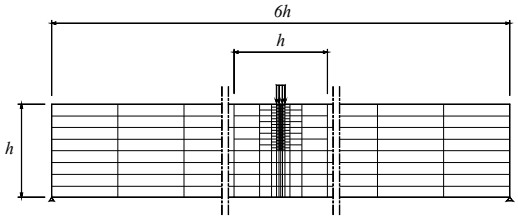

Figure 4. FE model of the adapted SEN-TPB.

A characteristic cohesive damage model (Figure 5) was used in the FEA to simulate damage initiation and growth in *Picea abies* L. wood using the set of cohesive parameters shown in Table 3 [4]. According to this damage model two different phenomena observed in wood are simulated regarding micro-cracking (first branch) and fibre-bridging (second branch). In the course of the loading process only the load-displacement data (Figure 6) is necessary to evaluate the *Resistance*-curve (*R*-curve). The performance of the method is assessed comparing the horizontal asymptote of the obtained *R*-curve (i.e., G_{Ic}) with the value used as input (G_{Ic}(inp)) in the cohesive damage model.

Table 2 – Elastic properties of *Picea abies* L [4].

E_L (MPa)	E_R (MPa)	E_T (MPa)	ν_{LT}	ν_{LR}	ν_{TR}	G_{TL} (MPa)	G_{RT} (MPa)	G_{RL} (MPa)
9 900	730	334	0.44	0.43	0.25	610	22	500

Table 3 –Cohesive properties of *Picea abies* [4].

f_t (MPa)	f_b (MPa)	w_b (mm)	G_{Ic} (N/mm)
1.660	0.300	0.090	0.145

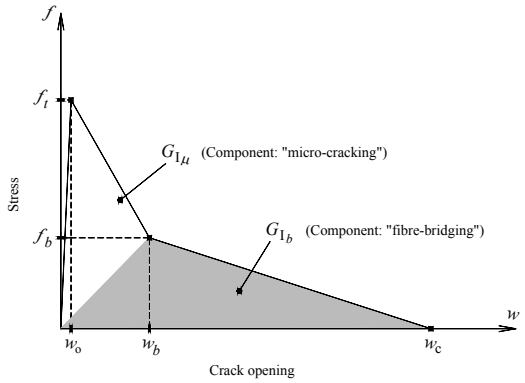

Figure 5. Bilinear damage law.

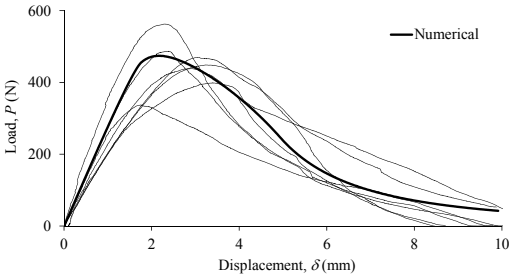

Figure 6. Load-displacement curves (D_4).

3. COMPLIANCE BASED BEAM METHOD

Wood fracture characterization is not feasible using the classical data reduction schemes. The reason for this is that crack length monitoring is required for those methods, which is impossible to achieve in wood. Indeed, since fracture in wood frequently involves micro cracking and fibre bridging, the definition of an undoubtable criterion to identify the crack tip is not viable. Additionally, the development of a non-negligible fracture process zone (FPZ) ahead of the visible crack free region is prematurely affected by the compressive stresses beyond the neutral axis [4]. This phenomenon hinders the self-similar crack propagation necessary to determine accurate values of fracture energy. Therefore, a method based on beam theory and equivalent crack concept is used to overcome the referred drawbacks, allowing the identification of adequate specimen sizes for the SEN-TPB.

An aspect that renders difficult the direct application of beam theory has to do with the presence of a material discontinuity (i.e., a crack) that affects the stress profile due to bending in the referred region. Following the suggestion of Kienzler and Herrmann [13] a triangular stress relief region (SRR) is used (Figure 7). In this domain normal stresses due to bending are thus drop to zero, which is considered in the evaluation of the strain energy due to bending,

$$U = 2\left[\int_0^{L_2} \frac{M_f^2}{2E_L I} dx + \int_{L_2}^{L_1} \frac{M_f^2}{2E_L I_{sr}} dx + \int_{L_1}^{L} \frac{M_f^2}{2E_T I_{sr}} dx\right] \quad (1)$$

with L_1 standing for the length of the lateral segments, M_f for the bending moment ($M_f = Px/2$) and E_L and E_T for the Young modulus in the longitudinal and transverse direction, respectively (Figure 3). Parameters I and I_{sr} are the second moment of area of the entire section (height h) and the effective section in the SRR (height $h(x)$), respectively (Figure 7),

$$I = \frac{bh^3}{12}\ ;\ I_{sr} = \frac{b\left[h(x)\right]^3}{12} \quad (2)$$

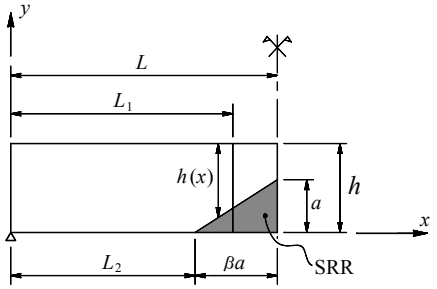

Figure 7. Specimen geometry and SRR.

with b standing for the specimen width. Therefore,

$$h(x) = h + \frac{a}{L - L_2}\left(L_2 - x\right) \quad (3)$$

with a being the crack length. By substituting Eqs. (2) and (3) in Eq. (1), and applying the Castigliano theorem,

$$\delta = \frac{\partial U}{\partial P} \quad (4)$$

the displacement δ is determined. As a consequence, the specimen compliance ($C = \delta/P$) turns,

$$C = \frac{2L_2^3}{E_L b h^3} + \frac{6(L-L_2)}{ba}\left\{\frac{1}{E_L}\left[\frac{L_1^2}{2\left(h(L_1)\right)^2} - \frac{L_2^2}{2h^2} + \frac{L-L_2}{a}\left(\frac{L_2}{h} - \frac{L_1}{h(L_1)}\right) + \left(\frac{L-L_2}{a}\right)^2 \ln\frac{h}{h(L_1)}\right] + \frac{1}{E_T}\left[\frac{L^2}{2(h-a)^2} - \frac{L_1^2}{2\left(h(L_1)\right)^2} + \frac{L-L_2}{a}\left(\frac{L_1}{h(L_1)} - \frac{L}{h-a}\right) + \left(\frac{L-L_2}{a}\right)^2 \ln\frac{h(L_1)}{h-a}\right]\right\} \quad (5)$$

In this equation $h(L_1)$ is determined from Eq. (3) considering $x = L_1$. Equation (5) does not take into account shear effects, which can be important for higher specimens. Wood is frequently affected by scatter in elastic properties [14], which can be observed in the value of E_T (Eq. 5). Therefore, potential inaccuracies can be corrected by considering a so-called flexural modulus (E_{Tf}), instead of the nominal value of E_T. This parameter is determined on the basis of the initial conditions, considering C_0 and a_0 in place of C and a, respectively. The value of E_L on the other hand has been considered negligible as demonstrated by Morel et al. [3] for this specimen geometry (Fig. 3).

As referred before crack length monitoring in wood is impossible to perform with accuracy. Instead, an equivalent value of this magnitude (a_e) is considered and defined as a function of the current compliance (C) by means of Eq. (5). This equivalent linear elastic fracture mechanics concept is restricted to materials that exhibit quasi-brittle failure like wood. Accordingly, the observed compliance modification is due to all the nonlinear phenomena associated to the FPZ development and/or crack propagation. As Eq. (5) does not provide an analytical solution for the equivalent crack length (a_e) for each point of the P-δ curve, it has to be solved numerically (bisection method). Therefore, using the Irwin-Kies equation,

$$G_I = \frac{P^2}{2b}\frac{dC}{da} \tag{6}$$

the strain energy release rate is obtained using a_e instead of a in Eq. (5),

$$G_I = \frac{3P^2(L-L_2)}{b^2}\left\{\frac{1}{E_L}\left[\frac{L_2^2}{2h^2a_e^2} - \frac{L_1^2(h+3ka_e)}{2a_e^2(h+ka_e)^3} + \right.\right.$$
$$+(L-L_2)\left(\frac{L_1(2h+3ka_e)}{a_e^3(h+ka_e)^2} - \frac{2L_2}{ha_e^3}\right) - \frac{(L-L_2)^2}{a_e^3}\left(\frac{3}{a_e}\ln\frac{h}{h+ka_e} + \frac{k}{h+ka_e}\right)\Bigg] +$$
$$+\frac{1}{E_{Tf}}\left[\frac{L^2(3a_e-h)}{2a_e^2(h-a_e)^3} + \frac{L_1^2(h+3ka_e)}{2a_e^2(h+ka_e)^3} - (L-L_2)\left(\frac{L_1(2h+3ka_e)}{a_e^2(h+ka_e)^2} + \frac{L(3a_e-2h)}{a_e^3(h-a_e)^2}\right) + \right.$$
$$\left.\left.+\frac{(L-L_2)^2}{a_e^3}\left(\frac{h(1+k)}{(h-a_e)(h+ka_e)} - \frac{3}{a_e}\ln\frac{h+ka_e}{h-a_e}\right)\right]\right\} \tag{7}$$

according which $k = (L_2\text{-}L_1)/(L\text{-}L_2)$. Hence, the R-curve is obtained without performing the crack length monitoring during the fracture test. The only parameter that has to be quantified is the extension of L_2.

4. RESULTS AND DISCUSSION

Cohesive zone modelling of six homothetic specimens (Table 1) was performed to investigate the specimen dimensions that provide the adequate replication of the G_{Ic} value used as input (i.e., G_{Ic}(inp)) in the plateau of the R-curve. In this computation the estimate of L_2 was necessary.

In this calculation the horizontal cathetus of the SRR (Figure 7) was determined considering the linear relation $\beta a = L\text{-}L_2$, being β a constant that has to be determined numerically. As observed in Figure 7, as the crack length a advances the ligament length (i.e., h-a) decreases, which leads to the decrease of L_2.

Figures 8(a-e) show the evaluated R-curves for specimen sizes D_0 to D_4 (Table 1), using the compliance beam based method detailed in Section 3. In these figures the strain energy release rate was normalized by the value of (G_{Ic}(inp)) used as input. For each R-curve the value of β rendering possible the attainment of a horizontal asymptote equal to the unity is included. The sequence of plots shows that β converges to 1.07 for specimen sizes higher than 70 mm (i.e., series D_2 in Table 1). The plotting of series D_5 is not made since it exhibits the same trend. In fact, as observed in [4] the ligament length and the extent of the FPZ may induce spurious effects, thus affecting the R-curve. Indeed, the normal compressive stresses induced by bending impede crack propagation in a self-similar way after a given extent. In the case that the ligament length is not sufficient a plateau is not revealed and the critical energy release rate (G_{Ic}) is not possible to determine. Figures 8 (a-e) also show the evolution of the cohesive zone (CZ) extent with the equivalent crack length normalized by the initial ligament length. It is possible to observe that the extent of the CZ provides an alternative way to verify whether the self-similar crack propagation has occurred in the SEN-TPB. It is clear that a undoubtable plateau both on the *Resistance* to crack growth and the CZ extent is revealed for specimen sizes higher that 140 mm (i.e., series D_3 in Table 1). Also, the CZ confinement permits to observe what is at the origin of the size effect phenomenon of quasi-brittle materials, i.e., the effect of the structure size on its nominal strength and on its resistance to crack growth at the peak load [15, 16].

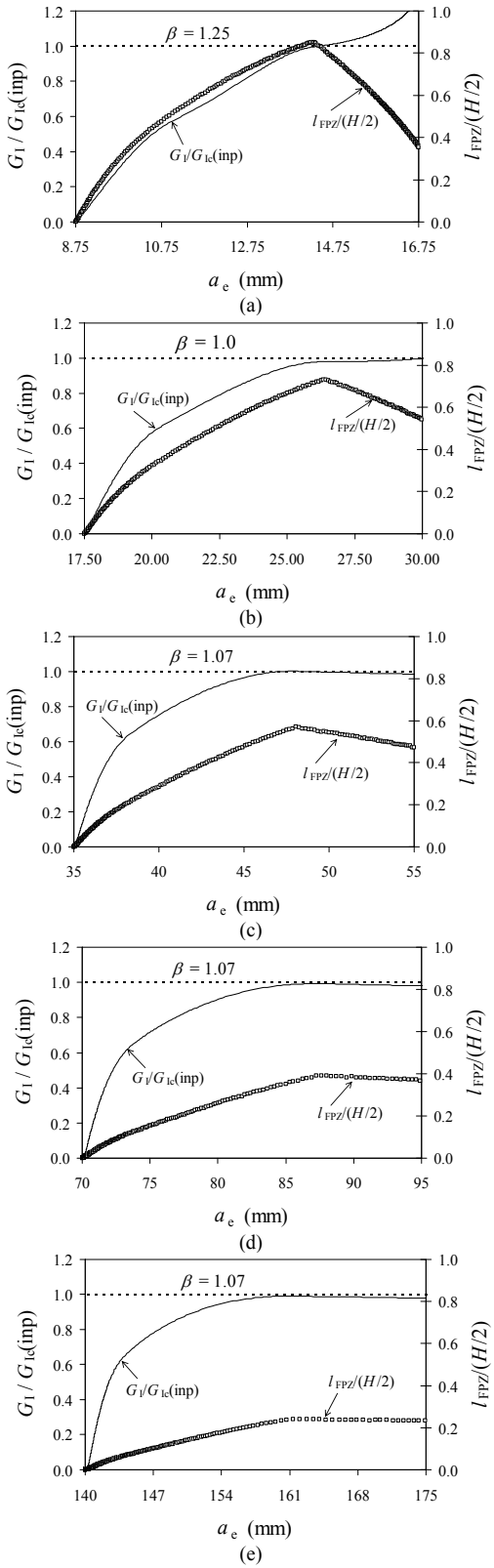

Figure 8. *R*-curves obtained for series: (a) D_0, (b) D_1, (c) D_2, (d) D_3 and (e) D_4.

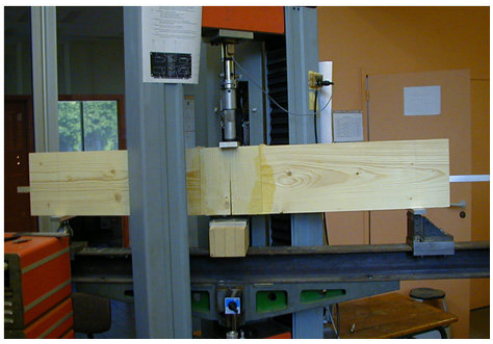

Figure 9. Set-up of the SEN-TPB test.

Figure 6 exhibits a total of seven P-δ curves obtained for series D_4, presenting h = 280 mm (i.e., higher than 140 mm). In the experiments (Figure 9) a load cell with the capacity of 1 kN has been installed and crosshead displacement rate regulated to reach the peak load P_u in 3±1 minute during fracture tests, thus minimizing possible viscoelastic effects in wood. The pronounced linear behaviour observed in the P-δ curves reveals that a non-negligible FPZ develops ahead of the crack tip. This phenomenon being a characteristic of quasi-brittle materials as wood leads to a pronounced *R*-curve. This may be confirmed by analysing Figure 10 for the corresponding data. Following an initial domain characterized by the development of the FPZ, the energy release rate tends to a horizontal asymptote, which gives the G_{Ic}.

The set of results presented in Table 4 show the initial compliance (C_0), the ultimate load (P_u), the critical crack length (a_c) and the critical energy release rate (G_{Ic}) obtained for the tested series. This set of results allows observing that the scatter is lower than 20% for the totality of the parameters, which reveals the quality of the results.

The value of a_c was obtained from the abscissa of the *R*-curve in the early stage of the plateau. Together with the initial crack length a_0, this parameter allows estimating an equivalent measure of the FPZ by doing $l_{FPZ} = a_c - a_0$ (i.e., 68 mm for series D_4). Table 4 also revealed that the critical energy release rate is equal to 0.219 N/mm.

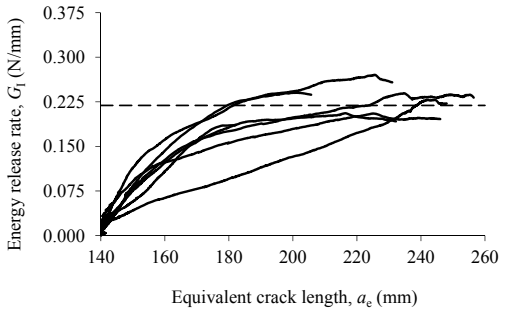

Figure 10. *R*-curves obtained for series D_4.

Table 4. Resume of experimental data (series D_4).

Specimen	C_0 (mm/N)	P_u (N)	a_c (mm)	G_{Ic} (N/mm)
1	0.00363	487	214	0.196
2	0.00498	399	177	0.185
3	0.00379	337	239	0.222
4	0.00494	470	210	0.262
5	0.00427	439	191	0.196
6	0.0027	563	229	0.232
7	0.00475	449	197	0.240
Average	0.00405	472	208	0.219
CoV	20%	19%	10%	13%

5. CONCLUSIONS

Mode I fracture characterization of wood was performed using a method based on beam theory and crack equivalent concept applied to the Single Edge Notched-Three Point Bending (SEN-TPB) that takes into account the presence of a stress relief region of triangular shape. The method dispenses the monitoring of the crack length during propagation, which is impossible to perform in wood.

Cohesive zone modelling was executed to mimic damage initiation and growth considering a set of six homothetic specimens. The simulations were performed using a set of characteristic cohesive parameters obtained in a previous work for *Picea abies* L. The objective was to verify whether the method used to evaluate the *Resistance*-curve was able to replicate the value of the fracture energy release rate that had been used as input, thus validating the procedure.

The used methodology presents the advantage that only requires the load-displacement data to evaluate the *Resistance*-curve. It was verified that the value of fracture energy is well captured in the plateau sector of the *Resistance*-curve, except for specimens of smaller dimensions characterized by the absence of a clear plateau. In regard to higher specimens, a constant value for the parameter that defines the cathetus of the stress relief zone was possible to obtain. Based on the results issued from the cohesive zone modelling a critical specimen size was identified for the SEN-TPB.
The procedure was then applied to experimental data considering a specimen with a convenient height. Consistent results have been obtained regarding the *Resistance*-curves.

Finally, it should be noted that the presented methodology is not exclusive for wood and that it can be easily applied to mode I fracture characterization of other materials using this test.

REFERENCES

[1] European Committee for Standardization (2004). EN 1995-1-1 Design of timber structures. Part General rules and rules for buildings. Brussels.
[2] Stanzl-Tschegg SE, Tan DM, Tschegg EK. New splitting method for wood fracture characterization. Wood Science and Technology 1995; 29:31–50.
[3] Morel S, Dourado N, Valentin G, Morais J. Wood: a quasibrittle material - R-curve behavior and peak load evaluation. International Journal of Fracture 2005; 131:385–400.
[4] Dourado N, Morel S, de Moura MFSF, Valentin G, Morais J. Comparison of fracture properties of two wood species through cohesive crack simulations. Composites Part A 2008; 39 415–27.
[5] de Moura MFSF, Morais J, Dourado N. A new data reduction scheme for mode I wood fracture characterization using the double cantilever beam test. Engineering Fracture Mechanics 2008; 75:3852-65
[6] Yoshihara H, Kawamura T. Mode I fracture toughness estimation of wood by DCB test. Composites Part A 2006; 37: 2105–13.

[7] Boström L. The stress-displacement relation of wood perpendicular to the grain. Wood Science and Technology 1994; 28:319-27.
[8] Gustafsson PJ (1988). A study of strength of notched beams. Paper 21-10-1. In: Proceedings of CIB-W18A Meeting, Parksville, Canada.
[9] Daudeville L. Fracture in spruce: experiment and numerical analysis by linear and non linear fracture mechanics, Holz als Roh und Werkstoff 1999; 57: 425-32.
[10] Dourado N (2008). R-Curve behaviour and size effect of a quasibrittle material: Wood. PhD Thesis. University of Trás-os-Montes Alto Douro and University of Bordeaux I (Under Co-tutorship). Vila Real. Portugal.
[11] Petersson PE. Crack growth and development of fracture zone in plain concrete and similar materials. Report No. TVBM-1006, Division of Building Materials, Lund Institute of Technology, Lund, Sweden; 1981.
[12] Guitard D. Mécanique du matériau bois et composites. Cepadues-Editions. ISBN 2.85428.152.7: 108-23¸1987.
[13] Kienzler R, Herrmann G. An elementary theory of defective beams. Acta Mech, 1986; 62:37-46.
[14] de Moura MFSF, Silva MAL, Morais J, de Morais AB, Lousada JJL. Data reduction scheme for measuring GIIc of wood in End-Notched Flexure (ENF) tests. Holzforschung 2009; 63:99-106.
[15] Bazant ZP. Scaling theory for quasibrittle structural failure. Proceedings of National Academy of Sciences 2007; 101:13400-13407.
[16] Morel S. R-curve and size effect in quasibrittle fractures: Case of notched structures. International Journal of Solids and Structures 2007; 44:4272–4290.